08

Sensitization of ZnO nanorods by $AgInS_2$ colloidal quantum dots for adsorption gas sensors with light activation

© A.A. Ryabko,[1,2] S.S. Nalimova,[1] D.S. Mazing,[1] O.A. Korepanov,[1] A.M. Guketlov,[3] O.A. Aleksandrova ,[1] A.I. Maximov,[1] V.A. Moshnikov,[1] Z.V. Shomakhov,[3] A.N. Aleshin[2]

[1] St. Petersburg State Electrotechnical University LETI, St. Petersburg, Russia
[2] Ioffe Institute, St. Petersburg, Russia
[3] Kabardino-Balkarian State University, Nalchik, Russia
e-mail: a.a.ryabko93@yandex.ru

Received January 21, 2022
Revised March 13, 2022
Accepted March 14, 2022

A low-temperature technique for the formation of coatings based on ZnO nanorods decorated with colloidal $AgInS_2$ quantum dots is presented. It is shown that ZnO nanocrystals and colloidal $AgInS_2$ quantum dots with a shell of mercaptopropionic acid molecules form a heterojunction. Sensitization of ZnO nanorods with $AgInS_2$ colloidal quantum dots to visible irradiation provides a gas analytical response of the structure to isopropyl alcohol vapor at room temperature under blue LED illumination with a peak wavelength of 460 nm.

Keywords: adsorption gas sensors, photoactivation of gas sensitivity, zinc oxide nanorods, $AgInS_2$ colloidal quantum dots, sensitization.

DOI: 10.21883/TP.2022.06.54418.15-22

Introduction

An operating principle of the adsorption gas sensors (chemiresistive gas sensors) is based on changing the electrical resistance of the sensitive material as a result of the chemical reaction with a gas agent on its surface. The sensitive materials for the adsorption sensors include a wide class of materials comprising metal oxides [1–6], nitrides [7–10] and sulfides [11,12], carbon nanomaterials [13–16], conductive polymers [17–19], 2*D*-materials [20,21], etc. Nevertheless, it is metal oxides, combinations and compositions thereof that are intensely studied and applied in practice in the adsorption gas sensors. Despite that the adsorption gas sensors have a lot of advantages such as high sensitivity, miniaturizability of a sensor element, and low fabrication cost, their wide application in portable devices is limited by high operating temperatures (200−500°C). The high-temperature operation of the sensor element is accompanied by such problems as high energy consumption, necessity of heat removal, reduction of the service life of the sensor element, as well as risks of operating in an explosive atmosphere [22]. Presently, the said problems are solved by developing the adsorption gas sensors based on the metal oxides, which operate at lower temperature, i.e. at the room temperature [23–27].

In order to activate gas sensitivity of the layers of nanostructured metal oxides at the room temperature, optical generation of free charge carriers is used instead of heating. The most of the metal oxides used are wide-bandgap semiconductors, and they are irradiated in the ultraviolet range [28–33]. In order to extend the light absorption range for photoactivation of gas sensitivity to the long-wave range, a wide number of the studies is performed to decorate the metal oxides with more narrow-band semiconductors, for example, CdSe [34], CdS [35], PbS [36,37], g-C_3N_4 [38], rGO [39].

The present study is to investigate decoration of the zinc oxide nanorods (NR) with $AgInS_2$ colloidal quantum dots (CQDs) to be used in the adsorption gas sensors with the optical activation. The zinc oxide nanorods are considered to be a bio-compatible material with low toxicity [40,41]. In turn, the $AgInS_2$ CQDs are neither composed of heavy metals and are a lower toxic analogue of binary chalcogenides. The $AgInS_2$ colloidal dots are studied to be applied as marks of biological markers [42] as well as for sensitization of photocatalysts to visible light [43,44].

The present study synthesizes the zinc oxide nanorods and the $AgInS_2$ CQDs at relatively low temperatures. This approach provides for environmental safety and reduces energy consumption of the technological processes, in which the gas-sensitive coating is created based on the zinc oxide nanorods and the $AgInS_2$ CQDs for the adsorption gas sensors with optical activation. It is found that the zinc oxide nanocrystals and the $AgInS_2$ CQDs form a heterojunction. The zinc oxide nanorods are decorated with the $AgInS_2$ quantum dots to increase the NR photoconductivity in the visible range, thereby ensuring the sensitivity of the ZnO NRs to isopropyl alcohol vapors at the room temperature under conditions of irradiation with blue light.

1. Materials and research techniques

The ZnO NR coatings were synthesized on various substrates in two stages: depositing a nucleating layer by the ultrasound spray-pyrolysis method and growing the NRs

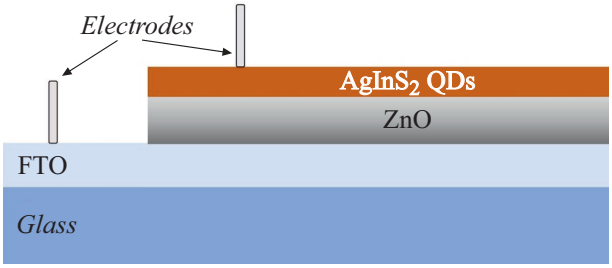

Figure 1. Structure based on zinc oxide and CQDs to record the photovoltaic effect.

by the soft hydrothermal method [45]. After the ZnO NRs had been synthesized, the samples were annealed at the temperature of 500°C for 10 min. In order to analyze the samples by means of the X-ray photoelectron spectroscopy, the synthesis was performed on silicon substrates, while for recording the photovoltaic effect — on glass substrates with the FTO coating (tin oxide alloyed with fluorine). In order to record a photoresponse and gas sensitivity, the samples were synthesized on ceramic substrates with interdigital electrodes (NiCr/Ni/Au). The width of the electrodes and the distance between them was 25 μm.

The $AgInS_2$ CQDs stabilized by the mercaptopropionic acid were synthesized by a procedure based on data of the study [46]. The mercaptopropionic acid was selected to be ligand-stabilizers due to its relatively short molecule, thereby ensuring transportability of free charge carriers both between the CQDs, and from the CQDs to the NRs [47]. The colloidal solution was synthesized by solving 0.1 mmol of $AgNO_3$ and 2 mmol of the mercaptopropionic acid in 5 ml of distilled water. 50 μl of the 25% NH_4OH aqueous solution and the 0.7 mmol of the $In(NO_3)_3 \cdot 4.5H_2O$ aqueous solution were added to the produced solution. The fast injection of 1 mmol of $Na_2S \cdot 9H_2O$ into the cation precursor solution resulted in instantaneous nucleation. The particles were grown for 30 min at the temperature of 95–100°C. The typical samples of the synthesized colloidal quantum dots are characterized in the studies [48,49]. The produced solution of the $AgInS_2$ CQDs was purified by adding isopropyl alcohol as a precipitant to be subsequently centrifuged. After the two purification cycles, the CQDs were dispersed into 1 ml of distilled water.

In order to record formation of the heterostructure between the zinc oxide and the $AgInS_2$ CQDs and, therefore, separability of the free charge carriers at the boundary thereof, a structure was formed based on the ZnO thin layer obtained by the spray-pyrolysis and the CQDs (Fig. 1), to subsequently measure its current-voltage curve, the short-circuit current and no-load voltage with light on.

The $AgInS_2$ CQDs were applied by centrifugation (2000 rpm) with subsequent heating ($\sim$ 80°C). The electrode on the CQD layer was formed by means of the carbon paste (SPI), while the electrode on the FTO-layer was made by means of silver paste (SPI). For the similar structure using the zinc oxide nanorods, the short-circuit current with light on was recorded. Pressure golden contacts were used as the electrodes. The photoresponse and the gas sensitivity of the sensitized NRs were investigated by a selected method of applying a uniform coating of separate parts to the NRs, which do not cover the zinc oxide surface. The methods included immersion of the samples into the sol of the $AgInS_2$ quantum dots for 15 h. Then, the samples were dried in air at the room temperature. Just prior to measuring the photoresponse and the gas sensitivity, they were dried at the temperature of 120°C for 30 min.

The chemical composition of the surface of the zinc oxide NRs before and after sensitization of the $AgInS_2$ CQDs was analyzed by the X-ray photoelectron spectroscopy (K-Alpha, Thermo Scientific). The survey spectra used to determine all available elements in the samples were obtained with the bond energy range from 0 to 1350 eV using the AlK_α X-ray radiation with the photon energy of 1486.6 eV. The surface charge was adjusted by a position of the $C1s$ peak at the bond energy of 284.6 eV [50].

The photoresponse and the gas sensitivity of the zinc oxide NRs to isopropyl alcohol vapors before and after sensitization were analyzed in the measurement cell with the possibility of LED light on the sample. The irradiation source was selected among the standard color LEDs to be a blue LED with the peak wave length of 460 nm (with the consumed power 70 mW) due to the largest overlapping of the luminescence spectra with the absorption spectrum of the $AgInS_2$ colloidal quantum dots (Fig. 2).

The current through the sample was measured using the Keithley 6485 picoammeter at the voltage of 5 V. The concentration of the isopropyl alcohol vapors of 1000 ppm was controlled by velocities of the fluxes of the carrier gas (dried air) and the isopropyl alcohol, which is described in detail in the study [51].

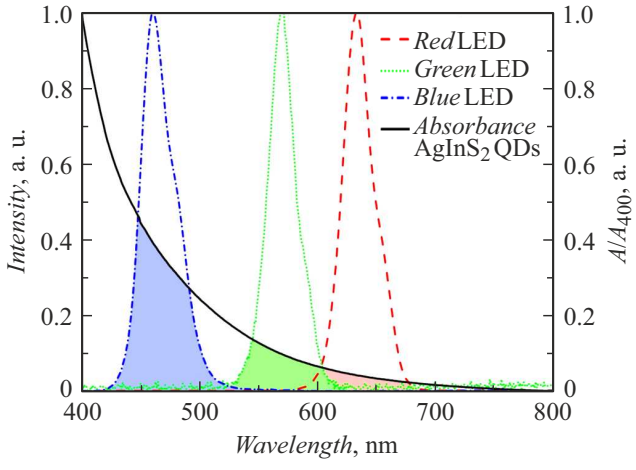

Figure 2. Spectra of luminescence of the LEDs and the absorption (absorbance) spectrum of the $AgInS_2$ CQDs.

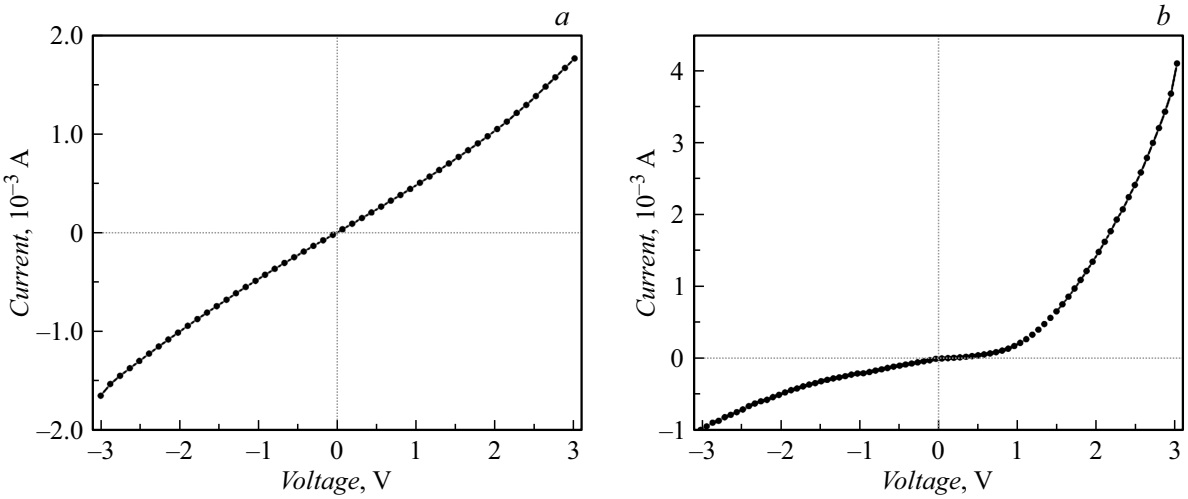

Figure 3. Current-voltage characteristics of the structures: *a* — FTO/ZnO, *b* — FTO/ZnO/ of the $AgInS_2$ CQDs. The area of the electrodes to the structures was different in the measurements.

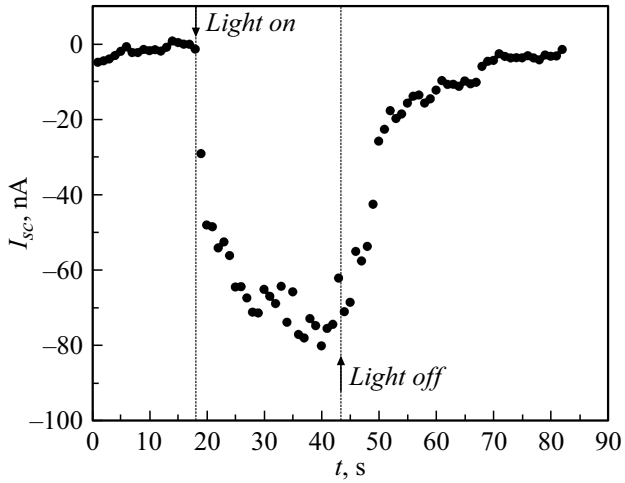

Figure 4. Recording the short-circuit current in FTO/NRs ZnO/$AgInS_2$ CQDs during irradiation.

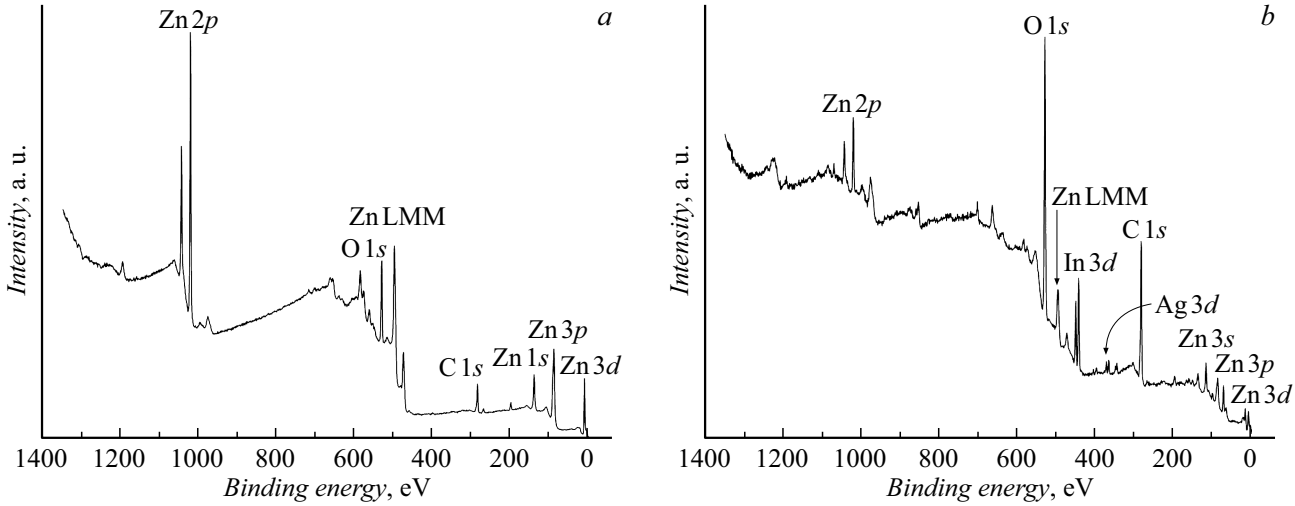

Figure 5. X-ray photoelectron spectra of the ZnO NRs (*a*) and the ZnO NRs decorated by the CQDs (*b*).

2. Results and discussion

The current-voltage curve (Fig. 3) measured for the formed structure FTO/ZnO/$AgInS_2$ CQDs is non-linear, and the current through the structure when a positive voltage is applied exceeds the reverse current. When irradiating the structure with a xenon lamp having a light filter (to block the ultra-violet radiation), the open-circuit voltage was several millivolts, while the short-circuit current was tens of nA. The current-voltage characteristic of the structure without the CQDs is linear.

Registration of the open-circuit voltage and the short-circuit current with light on and a rectification nature of the current-voltage curve of the structure FTO/ZnO/ $AgInS_2$ CQDs indicate that the ZnO/$AgInS_2$ CQDs heterostructure is formed and the photo-excited charge carriers are separated. The insignificant open-circuit voltage and the high reverse current may be due to both to a small difference in the work function of the ZnO polycrystal layer and the layer of the $AgInS_2$ CQDs, and to a significant concentration of trap states near the CQD surface and at the interlayer interface [52]. The characteristics are also affected by the material of the anode and the interface between the anode and CQD layer [47,53]. The registration of the short-circuit current with light on the structure with the ZnO NR coating (Fig. 4) also indicates the formation of the heterojunction at the interface ZnO NRs / $AgInS_2$ CQDs.

Thus, it can be said that the zinc oxide NRs and the layer of the $AgInS_2$ CQDs with a shell of mercaptopropionic acid form the heterojunction, which ensures the separation of the photo-excited charge carriers. Therefore, decoration of the ZnO NRs by the $AgInS_2$ CQDs can provide for sensitization of the zinc oxide NRs to irradiation within the visible (> 380 nm) range of the spectrum.

The results of the X-ray photoelectron spectroscopy (XPS) of the ZnO NR coating are shown on Fig. 5, *a*. The sample surface has evident peaks, which correspond to zinc, oxygen and carbon. The survey X-ray photoelectron spectrum of the zinc oxide NRs modified by the $AgInS_2$ CQDs by immersion is shown on Fig. 5, *b*.

The surface of the CQD-modified NRs is analyzed with a result indicative of the presence of zinc, oxygen, carbon, indium and silver. The sulphur peak intensity is comparable with the background noise of the spectrum. Thus, it is impossible to unambiguously make a conclusion about presence of sulphur on the surface from the XPS data. The peaks $Ag3d_{5/2}$ and $Ag3d_{3/2}$ are observed at the binding energies of 373.6 and 367.6 eV, which corresponds to the Ag^+ cations in the $AgInS_2$ compound. The $In3d_{5/2}$ peak is located at the binding energy of 452.6 eV, while the $In3d_{3/2}$ peak — at 445.1 eV. The positions of the peaks are different by 7.5 eV, which corresponds to the In^{3+} cations in the crystal structure [54,55]. Thus, it can be concluded from the panoramic XPS spectra that the $AgInS_2$ CQDs are adsorbed on the surface of the zinc oxide NRs, whereas a part of the surface of the ZnO NRs remains open. When comparing the survey spectra, there is also evident significant increase in the intensity of the peaks, which correspond to oxygen and carbon. It has also been detected that prior to decoration the spectrum of the O1s core level consisted in peaks corresponding to oxygen in the charged state O^{2-} (530.6 eV), i.e. oxygen in the ZnO crystal lattice, and to oxygen within the OH^- groups (531.7 eV) [56]. However, after decorating by the $AgInS_2$ QCDs, the O1s spectrum contained one peak corresponding to the binding energy of 531.3 eV. The change of the O1s spectrum indicates that the increase in the intensity of the peaks of oxygen and carbon is due to presence of molecules of the mercaptopropionic acid ($HSCH_2CH_2CO_2H$) on the sample surface.

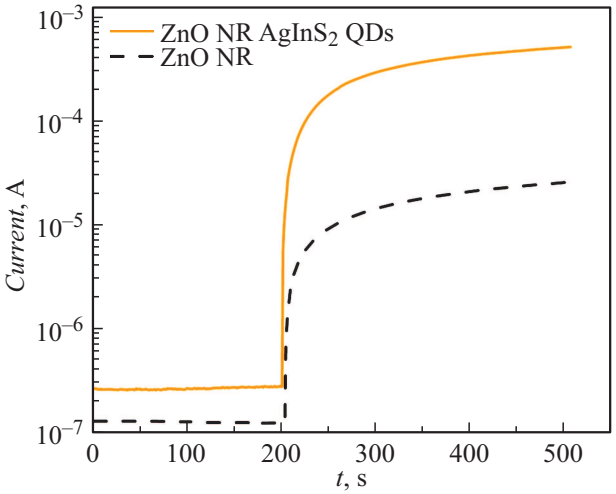

Figure 6. Current through the ZnO NR coating before and after decoration by the $AgInS_2$ QCDs in case of the blue-LED irradiation (460 nm). The irradiation has started after 200 s.

The photoresponse to the blue-LED irradiation of the NR coating before and after decoration by the $AgInS_2$ QCDs is shown on Fig. 6.

As it is clear from Fig. 6, the zinc oxide NRs have the photoconductivity in visible irradiation without decorating by the $AgInS_2$ QCDs, which is due to defect levels within an zinc oxide band gap ($E_g \approx 3.3$ eV) [45]. Nevertheless, NR decoration by the $AgInS_2$ QCDs results in increase in the photoresponse (I_{light}/I_{dark}) approximately in 10 times. There was no gas analytical NR response to the isopropyl alcohol vapors (at the concentrations up to 3000 ppm) without decorating by the $AgInS_2$ CQDs in blue-LED irradiation. The ZnO NR decoration by the $AgInS_2$ CQDs provides for the response of the coating to the isopropyl alcohol vapors in blue-LED irradiation at the room temperature (Fig. 7).

The gas analytical response (I_{gas}/I_{air}) of the sensitized ZnO nanorods to the isopropyl alcohol vapors with the concentration of 1000 ppm was 1.7. No response to the isopropyl alcohol vapors was recorded with light off. When irradiating the sensitized NRs, the photo-generated charge carriers (mostly in the $AgInS_2$ CQDs) are separated at the boundary of the heterojunction ZnO/$AgInS_2$, the lifetime of the charge carriers increases, so does the concentration of

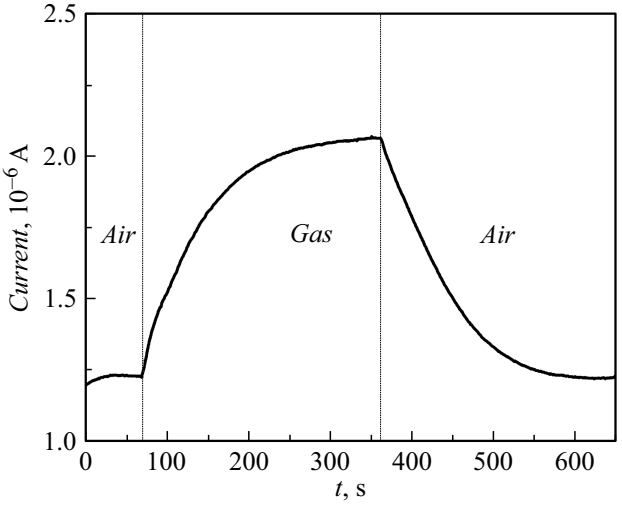

Figure 7. Time dependence of the current flowing through the coating ZnO NRs sensitized by the $AgInS_2$ colloidal dots, under impact of the isopropyl alcohol vapors with the concentration of 1000 ppm.

the zinc oxide electrons. The atmospheric oxygen molecules react with the photo-generated electrons, thereby resulting in formation of negatively charged oxygen ions and their adsorption on the ZnO NR surface:

$$O_2 + e^-(h\nu) \rightarrow O_2^-(h\nu).$$

The adsorption of the photo-induced charged ions $O_2^-(h\nu)$ on the ZnO NR surface results in formation of a depleted area. The photo-induced charged ions $O_2^-(h\nu)$ are weakly bonded to the ZnO surface and in the atmosphere of the isopropyl alcohol vapors interact with the alcohol molecules:

$$2C_3H_7OH + 9O_2^-(h\nu) \rightarrow 6CO_2 + 8H_2O + 9e^-.$$

In the course of the chemical reaction with the isopropyl alcohol molecules the electrons return to a conductivity band of the zinc oxide, while the depleted-charge area reduces on the NR surface and the ZnO NR conductivity increases. When supplying air, the oxygen molecules again adsorb on the surface with capturing the electrons out of the conductivity band, thereby resulting in recovery of the initial resistance. Thus, the ZnO NR decoration by the $AgInS_2$ CQDs allows sensitizing the NRs to the visible irradiation by increasing the visible absorption and separating the charge carriers at the heterojunction boundary and ensures the gas analytical response to the isopropyl alcohol vapors at the room temperature under the irradiation conditions.

Conclusion

The study describes the low-temperature procedure of forming the ZnO NR coatings decorated by the $AgInS_2$ CQDs. The XPS analysis has shown that the ZnO NR decoration by the $AgInS_2$ CQDs by immersion into the aqueous solution ensures their adsorption on the NR surface. It is demonstrated that the ZnO nanocrystals and the $AgInS_2$ CQDs with the shell of mercaptopropionic acid molecules form the heterojunction, while the NR decoration with the $AgInS_2$ CQDs ensures increase in the photoconductivity in the visible irradiation. The produced ZnO NR coatings decorated by the $AgInS_2$ CQDs show the 1.7 gas analysis response to the isopropyl alcohol vapors with the concentration of 1000 ppm under the illumination conditions at the room temperature. Thus, the ZnO NR sensitization by the $AgInS_2$ CQDs is effective for developing the gas-sensitive layers with photoactivation, which can operate at the room temperature in the dry air atmosphere.

Conflict of interest

The authors declare that they have no conflict of interest.

References

[1] V.A. Moshnikov, I.E. Gracheva, V.V. Kuznezov, A.I. Maximov, S.S. Karpova, A.A. Ponomareva. J. Non-Cryst. Solid., **356**, 37 (2010). DOI: 10.1016/j.jnoncrysol.2010.06.030
[2] S.S. Karpova, V.A. Moshnikov, S.V. Mjakin, E.S. Kolovangina. Semiconductors, **47** (3), 392 (2013). DOI: 10.1134/S1063782613030123
[3] S.S. Karpova, V.A. Moshnikov, A.I. Maksimov, S.V. Mjakin, N.E. Kazantseva. Semiconductors, **47**, 1026 (2013). DOI: 10.1134/S1063782613080095
[4] L.K. Krasteva, D.T. Dimitrov, K.I. Papazova, N.K. Nikolaev, T.V. Peshkova, N.V. Kaneva, V.A. Moshnikov, I.E. Gracheva, S.S. Karpova. Semiconductors, **47** (4), 586 (2013). 10.1134/S106378261
[5] D.T. Dimitrov, N.K. Nikolaev, K.I. Papazova, L.K. Krasteva, A.S. Bojinova, T.V. Peshkova, N.V. Kaneva, I.A. Pronin, I.A. Averin, N.D. Yakushova, A.A. Karmanov, A.T. Georgieva, V.A. Moshnikov. Appl. Surf. Sci., **392**, 95 (2017). DOI: 10.1016/j.apsusc.2016.08.049
[6] S. Mahajan, S. Jagtap. Appl. Mater. Today, **18**, 100483 (2020). DOI: 10.1016/j.apmt.2019.100483
[7] V.K. Tomer, R. Malik, A. Kailasam. ACS Omega, **2**, 3658 (2017). DOI: 10.1021/acsomega.7b00479
[8] C. Gautam, C.S. Tiwary, L.D. Machado, S. Jose, S. Ozden, S. Biradar, D.S. Galvao, R.K. Sonker, B.C. Yadav, R. Vajtaia, P.M. Ajayan. RSC Adv., **6**, 87888 (2016). DOI: 10.1039/C6RA18833H
[9] F. Qu, Y. Yuan, R. Guarecuco, M. Yang. Small, **12**, 3128 (2016). DOI: 10.1002/smll.201600422
[10] F. Qu, Y. Yuan, M. Yang. Chem. Mater., **29**, 969 (2017). DOI: 10.1021/acs.chemmater.6b03435
[11] L. Zhu, C. Feng, F. Li, D. Zhang, C. Li, Y. Wang, Y. Lin, S. Ruan, Z. Chen. RSC Adv., **4**, 61691 (2014). DOI: 10.1039/C4RA11010B
[12] S. Hussain, T. Liu, M. Javed, N. Aslam, W. Zeng. Sens. Act. B, **239**, 1243 (2017). DOI: 10.1016/j.snb.2016.09.128
[13] Q. Nie, W. Zhang, L. Wang, Z. Guo, C. Li, J. Yao, M. Li, D. Wu, L. Zhou. Sens. Act. B, **270**, 140 (2018). DOI: 10.1016/j.snb.2018.04.170

[14] M. Zhang, H.C. Su, Y. Rheem, C.M. Hangarter, N.V. Myung. J. Phys. Chem. C, **116**, 20067 (2012). DOI: 10.1021/jp305393c
[15] D.H. Shin, J.S. Lee, J. Jun, S.G. Kim, J. Jang. ACS Appl. Mater. Interfac., **7**, 1746 (2015). DOI: 10.1021/am507314t
[16] S. Mao, G. Lub, J. Chen. J. Mater. Chem. A, **2**, 5573 (2014). DOI: 10.1039/C3TA13823B
[17] T.N. Ly, S. Park. Sci. Reports, **8**, 18030 (2018). DOI: 10.1038/s41598-018-36468-z
[18] Y. Guo, T. Wang, F. Chen, X. Sun, X. Li, Z. Yu, P. Wan, X. Chen. Nanoscale, **8**, 12073 (2016). DOI: 10.1039/C6NR02540D
[19] H.T. Hien, H.T. Giang, N.V. Hieu, T. Trung, C.V. Tuan. Sens. Act. B, **249**, 348 (2017). DOI: 10.1016/j.snb.2017.04.115
[20] G.J. Choi, R.K. Mishra, J.S. Gwag. Mater. Lett., **264**, 127385 (2020). DOI: 10.1016/j.matlet.2020.127385
[21] O. Faye, U. Eduok, J.A. Szpunar, A.C. Beye. Physica E, **117**, 113794 (2020). DOI: 10.1016/j.physe.2019.113794
[22] J. Wang, S. Fan, Y. Xia, C. Yang, S. Komarneni. J. Hazard. Mater., **381**, 120919 (2020). DOI: 10.1016/j.jhazmat.2019.120919
[23] Y. Gui, K. Tian, J. Liu, L. Yang, H. Zhang, Y. Wang. J. Hazard. Mater., **380**, 120876 (2019). DOI: 10.1016/j.jhazmat.2019.120876
[24] H. Ma, L. Yu, X. Yuan, Y. Li, C. Li, M. Yin, X. Fan. J. Alloys Compounds, **782**, 1121 (2019). DOI: 10.1016/j.jallcom.2018.12.180
[25] M. Wang, Y. Zhu, D. Meng, K. Wang, C. Wang. Mater. Lett., **277**, 128372 (2020). https://doi.org/10.1016/j.matlet.2020.12837
[26] A.A. Bobkov, D.S. Mazing, A.A. Ryabko, S.S. Nalimova, A.A. Semenova, A.I. Maksimov, E.A. Levkevich, V.A. Moshnikov. 2018 Proceed. IEEE Intern. Conf. Electr. Eng. Photon., EExPolytech., 219 (2018). DOI: 10.1109/EExPolytech.2018.8564407
[27] S.S. Nalimova, V.M. Kondratev, A.A. Ryabko, A.I. Maksimov, V.A. Moshnikov. J. Phys. Conf. Series, **1658**, 012033 (2020). DOI: 10.1088/1742-6596/1658/1/012033
[28] Y.-T. Tsai, S.-J. Chang, L.-W. Ji, Y.-J. Hsiao, I-T. Tang, H.-Y. Lu, Y.-L. Chu. ACS Omega, **3**, 13798 (2018). DOI: 10.1021/acsomega.8b01882
[29] E. Espid, F. Taghipour. Sens. Actuators B, **241**, 828 (2017). DOI: 10.1016/j.snb.2016.10.129
[30] J. Jiang, L. Shi, T. Xie, D. Wang, Y. Lin. Sens. Actuators B, **254**, 863 (2018). DOI: 10.1016/j.snb.2017.07.197
[31] A.A. Ryabko, S.S. Nalimova, A.I. Maximov, V.A. Moshnikov. Proceed. 2021 IEEE Conf. of Russ. Young Researchers in Electrical and Electronic Engineering, ElConRus, 1180 (2021). DOI: 10.1109/ElConRus51938.2021.9396166
[32] J. Prades, R. Jiménez-Díaz, F. Hernandez-Ramírez, S. Barth, A. Cirera, A. Romano-Rodríguez, S. Mathur, J.R. Morante. Sens. Act. B, **140**, 337 (2009). DOI: 10.1016/j.snb.2009.04.070
[33] J. Li, D. Gu, Y. Yang, H. Du, X. Li. Front. Mater., **6**, 158 (2019). DOI: 10.3389/fmats.2019.00158
[34] A. Chizhov, M. Rumyantseva, R. Vasiliev, D. Filatov, K. Drozdov, I. Krylov, A. Abakumov, A. Gaskov. Sens. Act. B, **205**, 305 (2014). DOI: 10.1016/j.snb.2014.08.091
[35] H. Li, J. Yoon, C. Lee, K. Lim, J. Yoon, J. Lee. Sens. Act. B, **255**, 2963 (2018). DOI: 10.1016/j.snb.2017.09.118
[36] D. Zhang, G. Dong, Y. Cao, Y. Zhang. J. Colloid Interface Sci., **528**, 184 (2018). DOI: 10.1016/j.jcis.2018.05.085
[37] R. Chen, J. Wang, Y. Xia, L. Xiang. Sens. Act. B, **255**, 2538 (2017). DOI: 10.1016/j.snb.2017.09.059
[38] H. Wang, J. Bai, M. Dai, K. Liu, Y. Liu, L. Zhou, F. Liu, F. Liu, Y. Gao, X. Yan, L. Geyu. Sens. Act. B, **304**, 127287 (2020). DOI: 10.1016/J.SNB.2019.127287
[39] X. Geng, J. You, J. Wang, C. Zhang. Mater. Chem. Phys., **191**, 114 (2017). DOI: 10.1016/j.matchemphys.2017.01.046
[40] J. Zhou, N. Xu, Z.L. Wang. Adv. Mater., **18**, 2432 (2006). DOI: 10.1002/adma.200600200
[41] S. Rackauskas, N. Barbero, C. Barolo, G. Viscardi. Nanomater., **7**, 381 (2017). DOI:10.3390/nano7110381
[42] R. Castro, R. Pásco, M. Saraiva, J. Santos, D. Ribeiro. Spectrochim. Acta Part A: Molec. Biomolec. Spectroscopy, **267**, 120592 (2022). DOI: 10.1016/j.saa.2021.120592
[43] P. Ganguly, S. Mathew, L. Clarizia, S. Kumar, A. Akande, S.J. Hinder, A. Breen, S.C. Pillai. ACS Omega, **5**, 406 (2020). DOI: 10.1021/acsomega.9b02907
[44] X. Zheng, Y. Mao, J. Wen, X. Fu, X. Liu. Nanomater., **9**, 1567 (2019). DOI: 10.3390/nano9111567
[45] A.A. Ryabko, A.I. Maximov, V.A. Moshnikov, E.I. Terukov, V.N. Verbitskii, V.S. Levitskii. Semiconductors, **54**, 1496 (2020). DOI: 10.1134/S1063782620110238
[46] A. Raevskaya, V. Lesnyak, D. Haubold, V. Dzhagan, O. Stroyuk, N. Gaponik, D.R. Zahn, A. Eychmüller. J. Phys. Chem. C, **121**, 9032 (2017). DOI: 10.1021/acs.jpcc.7b00849
[47] G.H. Carey, A.L. Abdelhady, Z. Ning, S.M. Thon, O.M. Bakr, E.H. Sargent. Chem. Rev., **115**, 12732 (2015). DOI: 10.1021/acs.chemrev.5b00063
[48] O.A. Korepanov, D.S. Mazing, O.A. Aleksandrova, V.A. Moshnikov, A.S. Komolov, E.F. Lazneva, D.A. Kirilenko. Phys. Solid State, **61** (12), 2326 (2019). DOI: 10.1134/S1063783419120217
[49] O.A. Alexandrova, Yu.V. Balakshin, A.D. Bol'shakov, V.M. Kondratiev, O.A. Korepanov, D.S. Masing, A.I. Maksimov, E.V. Maraeva, V.A. Moshnikov, E.N. Muratova, A.V. Nazarov, S.S. Nalimova, V.A. Nikonova, N.V. Permyakov, Yu.S. Reutov, A.A. Ryabko, A.V. Startseva, A.A. Shemukhin, *Nanochastitsy, nanosystemy i ikh primenenie. Formirovanie nanosystem dlya sensoriki i meditsiny* (SPETU „LETI", SPb, 2021), p. 9–51 (in Russian).
[50] P.-T. Hsieh, Y.-C. Chen, K.-S. Kao, C.-M. Wan. Appl. Phys. A, **90**, 317 (2008). DOI: 10.1007/s00339-007-4275-3
[51] S.S. Nalimova, A.A. Ryabko, A.I. Maximov, V. Moshnikov. J. Phys.: Conf. Ser., **1697**, 012128 (2020). DOI: 10.1088/1742-6596/1697/1/012128
[52] S. Zang, Y. Wang, W. Su, H. Zhu, G. Li, X. Zhang, Y. Liu. Phys. Status Solidi RRL, **10**, 745 (2016). DOI: 10.1002/pssr.201600220
[53] C.M. Chuang, P.R. Brown, V. Bulovic, M.G. Bawendi. Nat. Mater., **13**, 796 (2014). DOI: 10.1038/NMAT3984
[54] S. Peng, S. Zhang, S.G. Mhaisalkar, S. Ramakrishna. Phys. Chem. Chem. Phys., **14**, 8523 (2012). DOI: 10.1039/C2CP40848A
[55] Y. Yang, Y. Liu, B. Mao, B. Luo, K. Zhang, W. Wei, Z. Kang, W. Shi, S. Yuan. Catal. Lett., **149**, 1800 (2019). DOI: 10.1007/s10562-019-02718-6
[56] P.-T. Hsieh, Y.-C. Chen, K.-S. Kao, C.-M. Wang. Appl. Phys. A, **90**, 317 (2008). DOI: 10.1007/s00339-007-4275